2012 IEEE/RSJ International Conference on
Intelligent Robots and Systems
October 7-12, 2012. Vilamoura, Algarve, Portugal

LineScout Power Line Robot: Characterization of a UTM-30LX LIDAR System for Obstacle Detection

Nicolas Pouliot, Pierre-Luc Richard, and Serge Montambault
Hydro-Québec's Research Institute (IREQ)
Varennes, Québec, Canada
pouliot.nicolas@ireq.ca

***Abstract* – This paper presents the characterization of the Hokuyo UTM-30LX laser range finder applied to obstacle detection on power line conductors. First, an overview section defines requirements and explains why the UTM-30LX was selected for this application. Next, since there is no published characterization of this particular sensor's performance, a comprehensive set of experiments is described, both general tests and ones specific to the novel problem of scanning a power line conductor to detect where obstructions are present. It is then explained how the LIDAR can be mounted on the LineScout power line robot and what algorithm is used to detect obstacles ahead. Basic results obtained on a full-scale power line mock-up clearly demonstrate the potential of the approach.**

Keywords- Field robotics; telerobotics; power line inspection robot; LIDAR

I. INTRODUCTION

Power line inspection robots have come into being as aging electrical infrastructures require new means of inspection and maintenance [1]. A few experimental technologies have drawn the attention of power utilities seeking to leverage their potential for inspections. Among these initiatives, Hydro-Québec's LineScout remains the sole technology to have actually made its way into the operations of a few power utilities since 2006 (Figure 1). This robot rolls along energized power lines, carries various cameras and sensors, and performs simple repair tasks. When it encounters such obstacles as suspension clamps, spacer-dampers and aerial markers, it extends itself to grab the line on the opposite side and flips its wheels over the obstacle [2][3]. A 3-km field mission was recently reported in [4].

To minimize development time, facilitate implementation and achieve effective use in the field, it was decided that LineScout should be introduced as a teleoperated technology [5]. Indeed, that decision proved its value as experienced line maintenance personnel are kept in the control loop, managing the inspection campaign. After a few years of use and over 50 field deployments, this principle is to be pushed one step further, as the long-term goal of the work presented is to let the operator focus solely on inspection and maintenance tasks, leaving the robot to perform autonomously the tedious, repetitive task of *obstacle detection and crossing*.

Figure 1. LineScout robot inspecting a power line

This paper presents the key specifications and operating context that form the basis of a multi-phase project. Following a description of the research context, test results are presented assessing for the first time the performance of the Hokuyo UTM-30LX laser range finder (LIDAR). Some results are of general interest, while others focus on scanning cylindrical objects similar to those encountered in the power line environment. Lastly, tests run on full-scale power line mock-ups demonstrate the potential of the approach.

II. OVERVIEW AND SPECIFICATIONS

A. Power Line Component Scanning

Figure 2 gives a generic overview of tasks that can be attempted while sensing an environment. Interestingly, it appears that the scanning resolution required for tasks is inversely proportional to computing speed they require. Hence, good computing speed is more important than very high sensor resolution for obstacle detection and localization.

The environment where power line robots move is semi-structured since the linear supporting wire clearly limits the region where obstacles can be found. Although shapes,

materials and linear position along the wire are unknown, detection and localization can be simplified to uni-dimensional problems.

Wires themselves are stranded cables with aluminum strands on the outer layers that differ in diameter (16 to 50 mm), and in shine, which depends on age and lighting conditions. For obstacle detection on such cables, it is assumed that detecting a sudden diameter change (exceeding a given threshold) will suffice to state that an obstacle is present. Based on onboard GPS coordinates and wheel odometer reading, the location of the obstacle can then be determined.

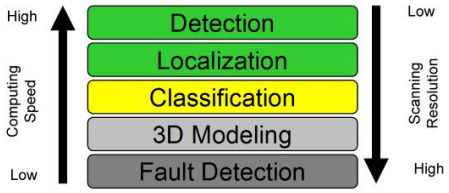

Figure 2. Environment scanning tasks for mobile robots

Throughout the world, a great variety of power line hardware components exists since numerous manufacturers compete. Also, infrastructure close to a century old means that components have been installed, repaired and replaced, not always in a well-documented way. That being said, the classification problem can typically be limited to a short list of component categories. The most common are shown in Figure 3 and include: aerial markers (3a, 3b) of different types and material; suspension clamps and insulator strings (3c), which support the conductor; vibration dampers (3d), installed near towers or at mid-span to damp wind-induced vibrations; spacer-dampers (3e), installed every 50 m or so on bundles of conductors to maintain spacing; and conductor splices (3f) to join ends during construction or to repair heavily damaged conductors.

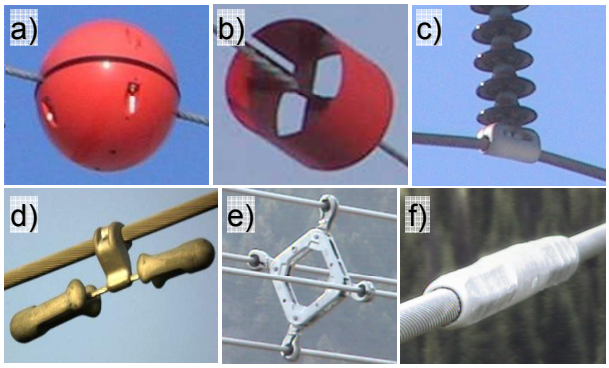

Figure 3. Categories of power line components

Provided sufficient resolution and information density are available, the next possibility is 3D modeling. This would allow a power utility to automatically build or update its field database. Ultimately, automated fault detection of line components could be achieved, using top-performing complimentary sensors. This paper limits the assessment to the initial steps, however, focusing on technologies that could quickly *detect* and *localize* power line components.

B. Survey of Proposed Solutions

Achieving obstacle detection and classification with a power line robot was proposed in 2002 by [6], using several arrays of ultrasonic proximity sensors. Data from the sensors is analyzed by a neural classification system. Using predefined thresholds, obstacles are classified and obstacle-crossing commands are simulated [7].

Image processing of video stream captured on transmission lines was presented in [8][9]. Using 2D feature detection, made easier by optimizing the camera angle to have a clear background, it was possible to discriminate between suspension clamps and dampers. Tests were successful in the laboratory and outdoors under proper lighting conditions.

Another interesting approach was presented in [10], where ultrasonic sensors and infrared imaging approaches were combined to leverage their complementary advantages.

A fourth type of technology was proposed more recently in [11][12]. It uses arrays of sensors to map the magnetic density around the aluminum alloy components of the power line in order to detect discontinuities caused by ferromagnetic components like vibration dampers and suspension clamps. It is not clear how the process is affected by the power line's fluctuating load current.

C. Rationale for Choosing the Hokuyo UTM-30LX

All four approaches mentioned above require considerable computing power, which is not necessarily available aboard LineScout given the choice to avoid onboard CPUs and hard drives for greater robustness and reliability. Transmitting raw data to the ground station, where sufficient processing power is available, would imply a large time delay. Also, some proposed methods have a very short detection range (a few centimeters), which would mean reduced LineScout traveling speed. Based on emergency braking tests performed at full speed (1 m/s) on a downward slope (15 deg.), the 110-kg LineScout could brought to a stop in 0.40 m. Assuming an acquisition period of 0.2 s and a computing time of 0.2 s, the minimum scanning distance was set to 0.9 m.

Another candidate sensor for the current application was the time-of-flight (TOF) camera, which has a good detection range but is sensitive to sunlight. Its 5-kg mass would bite heavily into the LineScout payload. Light-field cameras, and 3D stereo cameras were also dismissed due to their post-processing requirement.

Over the past 10 years, LIDAR has become a clear choice for a great number of mobile robotic applications. It is unmatched for several features: long detection range, simple computing and good acquisition speed. In recent years, its price has dropped, while resolution and robustness under outdoor conditions have improved. It is surprising that no other power line robots using LIDAR have yet been reported since manned aircraft equipped with such sensors are used to survey power line corridors in order to detect vegetation growth [13][14].

Among commercially available LIDAR sensors, the Hokuyo UTM-30LX was ultimately chosen as it offered the best compromise in terms of size, weight (370 g), power consumption (< 8 W) and resolution (0.25 deg.). In the 1-kg range, the IBEO Lux, SICK LD-MRS and SICK LMS 111 were also attractive, but bulkier, heavier and more expensive than the latest Hokuyo sensor.

III. *Characterization of the Hokuyo UTM-30LX*

Contrary to most earlier models of the Hokuyo family [15][16][17], formal characterization of the UTM-30LX has never before been presented. Some interesting papers have compared different LIDAR sensors to assess their performance in a specific context of operation [18][19]. The fact that a few authors have presented LIDAR applications involving scanning cylindrical features [20][21] was encouraging for the application at hand. Consequently, the objective of this paper is to assess the UTM-30LX's performance under various conditions that are specific to the power line environment. Hence, LIDAR warming, the effects of surface type, LIDAR orientation and distance to targets have been characterized in the 1-m range. Since the LIDAR is to scan cylindrical cables and various vibrating obstacles, a second series of tests focus on different types of cylindrical parts, seen at different distances and angles.

A. *Experimental Setup*

The setup consists of the LIDAR and a target, both mounted on a 1.6-m aluminum channel (Figure 4a).

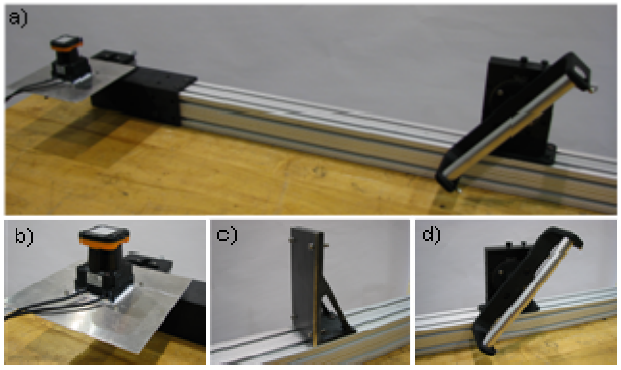

Figure 4. Experimental setup for LIDAR characterization

A micrometric stage allows transversal LIDAR positioning while the target is moved along the slots of the channel and positioned with a precision of 1.0 mm. As recommended by the manufacturer, an aluminum plate of 200 x 200 x 2 mm provides a heat sink for the LIDAR (Figure 4b). A thermal joint compound was used between the LIDAR and the plate to improve heat transfer. Figures 4c and 4d illustrate the two types of targets used in this study: plates and cylinders. The latter can be oriented with a precision of 0.5 degrees using a rotating table.

B. *Test Results*

This section presents the performances of the sensor in the aforementioned conditions. For comparison, as per manufacturer's specifications, sensor accuracy within a 10 m range and under 3000 lx, is 10 mm.

1) *Effect of Warming*

The first step of the characterization is to verify whether warming the LIDAR influences its output values. To do this, the flat plate was covered with a black sheet of paper and installed perpendicular to LIDAR, 1000 mm from it. This LIDAR has a scan angle of 270º divided into 1080 measurement steps. For this experiment, the distance given by step 182 was monitored for 120 minutes (3400 values).

Figure 5 presents data acquisition and data filtered using a moving average of 100 data points. The filtered curve shows that, using a proper heat sink, it takes the LIDAR about 60 minutes to reach a steady state at an ambient temperature of 22˚C. This may be explained by the warming of the motor spindle of the LIDAR [16]. All of the following tests were thus performed after more than 1 hour of operation. Note that after 30 minutes, though a steady state has not been reached, the relative error is already less than 0.3%, satisfactory for practical use of the LIDAR.

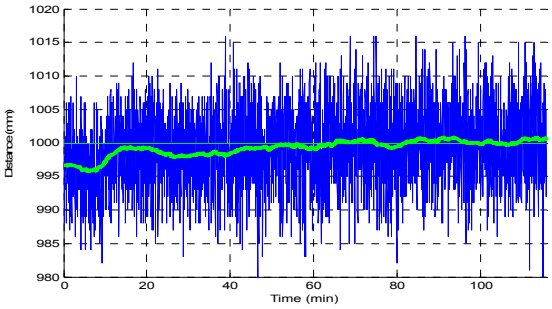

Figure 5. Effect of warming over time

2) *Effect of Surface Finish*

To see how the surface finish influences LIDAR measurements, three surfaces with distinct specular properties were tested perpendicular to the LIDAR and 1000 mm away: a polished aluminum plate (near-mirror finish), a black painted aluminum plate and the same black plate covered with a black sheet of paper. Each surface was scanned 2000 times.

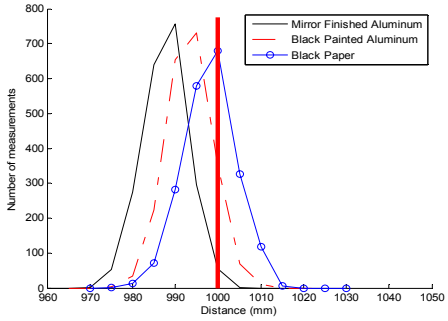

Figure 6. Effect of surface type on distance measurement

Figure 6 shows that the less a reflection on a surface is specular, the more accurate the distance measurement, as confirmed by the mean values: 989.7 mm, 995.3 mm and 999.9 mm respectively. Perpendicularity must also be taken

into account because the intensity of the returning laser beam is higher for specular surfaces perfectly perpendicular to the sensor, leading to slightly different distance measurements. However, the error remains quite small (< 1%) for the targets tested.

3) *Effect of Sensor Orientation*

The effect of the sensor's spatial orientation is crucial for this application since the LIDAR is to be installed on a mobile robot. While rolling along conductors, LineScout's orientation changes while obstacles are crossed and as it is pushed laterally by the wind. Its pitch varies roughly between -35˚ and +35˚, while its roll varies roughly between -10˚ and +10˚. The entire experimental setup in Figure 4a) (including the sensor and the target) was thus oriented horizontally, vertically, at a 45˚ angle and horizontally to the side (at 90˚ to the channel axis). Each test included 2000 measurements and mean values μ were computed and compared to reference distance D to get relative error ε:

$$|\varepsilon_i| = \left| \frac{\mu_i - D_i}{D_i} \right| \times 100 \qquad (1)$$

Where i represents a specific test, i.e. one of the four orientations described before.

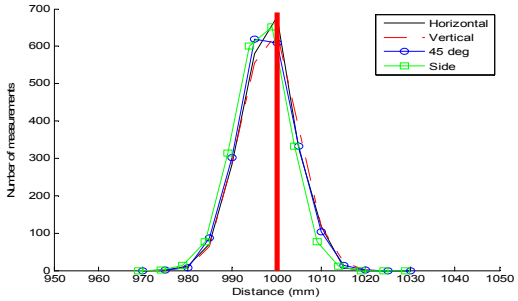

Figure 7. Effect of sensor orientation

This experiment revealed an important fact: the sensor's spatial orientation has no significant effect on the precision of measurements (see Figure 7). The relative error variation, given by $|\varepsilon_{max} - \varepsilon_{min}|$, was less than 0.14%. This suggests that this sensor is more robust than the one presented by [16]. Hence, this LIDAR can be installed and used for distance acquisition on a mobile robot like LineScout without significant loss in precision.

4) *Effect of Distance*

The effect of the distance between the target and the LIDAR is very important since it determines the position and orientation of the LIDAR on LineScout hence where on the conductors the LIDAR will point, i.e., how far in front the robot the LIDAR should scan. To assess the impact of distance on measurements, an initial series of tests were run with a black sheet of paper at three typical distances for the application: 500 mm, 1000 mm and 1500 mm. Obstacle detection is planned within these limits.

As shown by the curves in Figure 8, the standard deviation at the three distances remains within manufacturer specifications of 10 mm and does not vary significantly: 5.1 mm, 6.0 mm and 4.9 mm. Moreover, mean values are close to target values and errors ε for the three tested distances are all under 1.2% when scanning the zone of interest. An interesting result is that measurement at 1000 mm was most accurate. To verify this, tests with more representative targets were conducted and are presented in the following section.

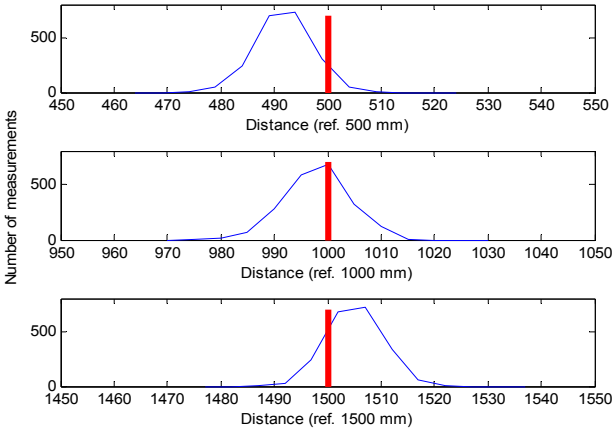

Figure 8. Effect of distance

5) *Performances with Cylindrical Targets*

Power line conductors are the main items to be scanned by the LIDAR. They have an unusual surface (twisted wires) and their surface finish is affected by aging. It is crucial to check UTM-30LX performance when scanning cylindrical parts with different surface finishes. Four targets were chosen with diameters between 25 and 28 mm, as illustrated in Figure 9a (from left to right): a polished aluminum rod, a white nylon rod, a clean cable and an aged cable with a rough and wavy surface. Figure 8b shows the major effect aging has on the cable surface (due to weather and pollution). A black sheet of paper wrapped around the aluminum rod provided a fifth target for testing.

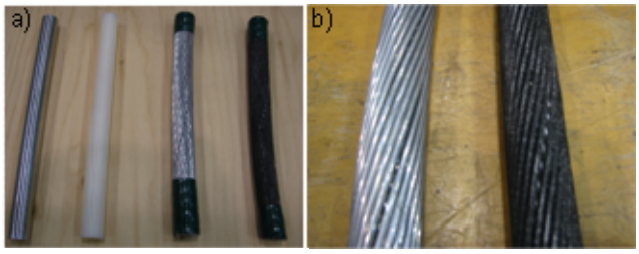

Figure 9. Cylindrical targets

a) *Effect of distance*

To better understand LIDAR distance measurements of cylindrical targets during LineScout inspections, a more realistic approach than monitoring a specific index was tested. Sections of targets were scanned completely and boundaries determined by calculating the maximum and minimum slopes from the data collected (distance vs. angle) near the targets. The center of each target was found and used to determine the closest point of the LIDAR (at which

the reference distances of the targets were set), and then compared to the reference distance. Mean distances and the associated error are listed in Table 1. Measurements are plotted in Figure 10.

Analysis of all results leads to the following very interesting observations:

1- Relative error from reference distances is generally low ($|\varepsilon| < 1.2\%$) for all targets except the white nylon rod. All standard deviations are between 4.8 and 6.3 mm.

2- Relative error is higher at short distances and tends to decrease with distance.

3- Distance measurements of aged cable are the most accurate at all three distances. Its irregular surface and rough, dark finish may explain this. Such results are promising for inspections, which will be performed by LineScout on aged cables. However, the error is satisfactory even for clean cable at 1000 mm or more.

4- Even though the targets were very unlike plates, some results from the earlier test (Section 4) are confirmed: distances are slightly underestimated at 500 mm and overestimated at 1500 mm (except for the nylon rod).

TABLE I. DISTANCE MEASUREMENT OF CYLINDRICAL TARGETS

Targets	500 mm		1000 mm		1500 mm	
	μ	ε	μ	ε	μ	ε
Aluminum	497,3	-0,5	1002,5	0,2	1504,5	0,3
White nylon	509,4	1,8	1016,5	1,6	1521,8	1,4
Clean cable	494,3	-1,2	1004,5	0,4	1504,8	0,3
Aged cable	497,5	-0,5	1001,5	0,1	1501,5	0,1
Black paper	494,3	-1,2	1005,2	0,5	1503,6	0,2

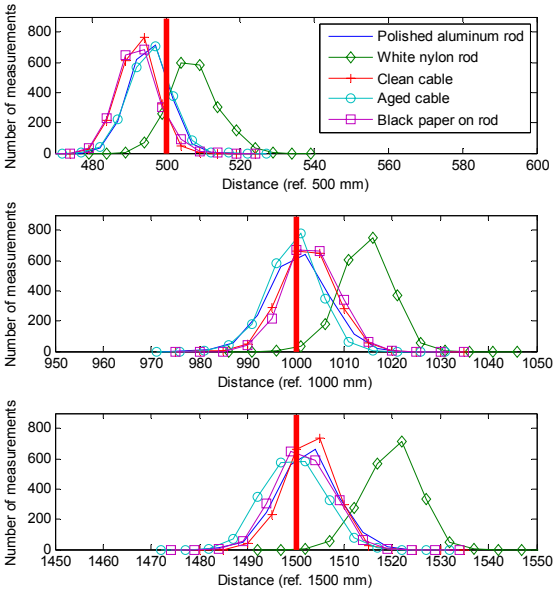

Figure 10. Effect of distance on the measurement of cylindrical targets

b) Effect of angle

It is necessary to scan conductors at an angle smaller than 90˚ (i.e., not perpendicularly) in order to detect obstacles in front of LineScout without placing the LIDAR on a long bracket. It is thus important to test cylindrical targets at different angles to determine the effect on precision. The cylindrical targets described above were positioned at 1000 mm and tested at four angles: 90˚, 65˚, 40˚ and 15˚. The results are presented in Figure 11. The cylindrical target was initially placed with its closest point (not its axis) at 1000 mm, so pivoting the target to a non-vertical angle progressively changes that distance.

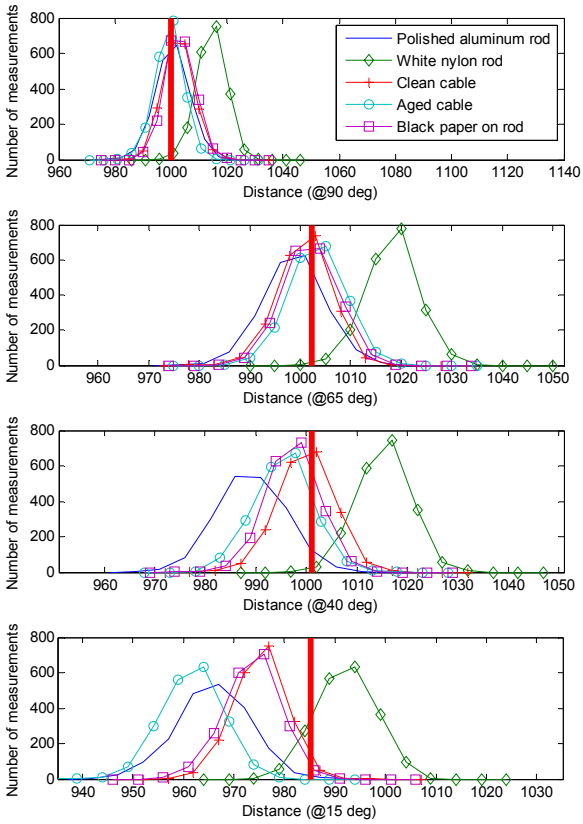

Figure 11. Effect of angle on the distance measurement

This test reveals that the error of distance measurements increases more significantly when the angle of incidence of the laser beam is far away from 90˚, while standard deviation is not significantly affected and remains within [4.9,7.1] mm. However, except for the nylon rod, keeping the angle greater than 15˚ limits the error ($|\varepsilon| < 1\%$). Angles of 15˚ and less can lead to a much greater error because the intensity of the reflected beam decreases with the angle, and may ultimately not be captured by the LIDAR ([15][16][17]). Note that for tests at 15˚, the precise evaluation of the reference distance is more sensible to the actual LIDAR scanning plane position, thus the precision of red line position is estimated to ±4 mm. Nevertheless, these results are interesting in the sense that they discriminate the different surface types (wavy and polished surfaces are more affected).

c) Effect of vibrations

As mentioned earlier, the UTM-30LX LIDAR will be mounted on LineScout, a mobile robot, for obstacle detection. The LIDAR will thus be subjected to vibrations

during operation. Such vibrations are generated in part by the robot itself as it rolls along the conductor but mainly are inevitably induced by wind on the conductor. Vibration frequency depends primarily on wind speed and wire diameter, and ranges from 5 to 20 Hz. The performance of the Hokuyo LIDAR under vibration conditions must thus be tested.

As shown in Figure 12, the UTM-30LX LIDAR was mounted on a Unholtz-Dickie 5PM shaker and subjected to different vibration frequencies at two amplitudes (2 mm and 5 mm, both peak-to-peak). All amplitudes and frequencies were calibrated using an oscilloscope linked to a Wenglor laser pointing to the top of the LIDAR.

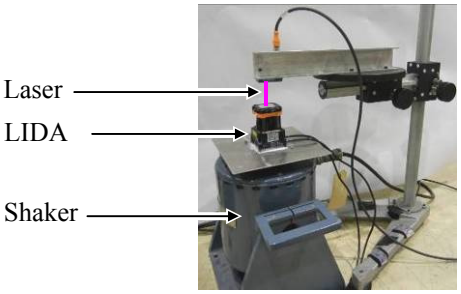

Figure 12. UTM-30LX vibration setup

Tests were performed on the clean cable target. Distance was evaluated as described earlier and the target scanned 2000 times. Figure 13 shows the results, which are very promising: vibration frequency does not significantly affect measurements. Relative error variation $|\varepsilon_{max} - \varepsilon_{min}|$ with frequency remains under 0.16% for an amplitude of 2 mm and 0.05% for 5 mm. Moreover, there is a slight difference between mean values at the two amplitudes. The authors believe that with the irregular surface of a cable composed of multiple strands, the laser beam hits another strand when oscillating with an amplitude of 5 mm and this leads to a greater variation in intensity due to the cylindrical surface of each strand.

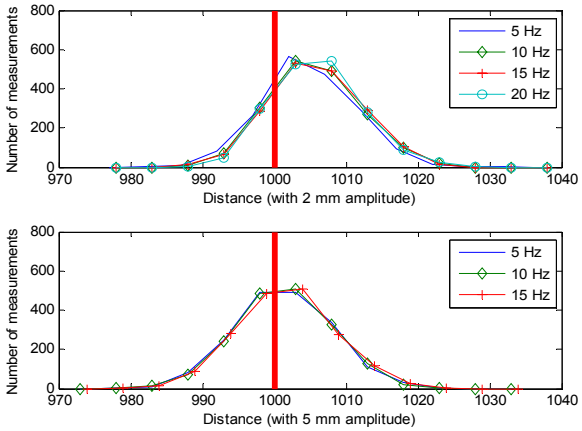

Figure 13. Effect of vibrations on the Hokuyo UTM-30LX

IV. *Preliminary Results on Power Line Mock-up*

The final objective of this study was to establish clearly the potential of the proposed method by using the Hokuyo LIDAR mounted on the LineScout platform and to assess realistically actual power line components.

A. Principle of Obstacle Detection

The proposed position and orientation for mounting the LIDAR are depicted in Figure 14. From the outset, it was decided that scanning would be upward to minimize the unwanted background and to better detect the variation in diameter due to an obstacle. This means a positive angle θ, and a location P_1 (LIDAR center point) below the conductor ($P_{1Z} < 0$) and in front of the front wheel ($P_{1X} > L$). Note that the positioning criteria could ultimately entail the use of two LIDARs, one for each direction of travel.

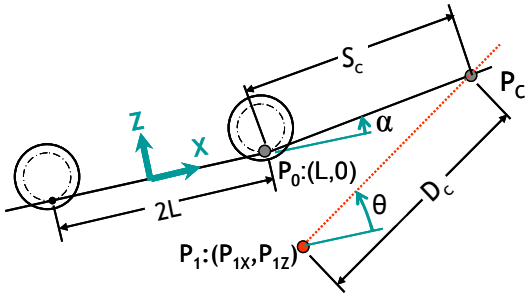

Figure 14. Positioning of the LIDAR on LineScout.

Although the obstacle must be detected at a sufficient distance (S_C > 0.9 m, see Section II C), pointing too far away along the conductor would mean that the LIDAR would scan the conductor's surface at too small an angle (θ ≤ 40º, see Section III B 5).

It was initially assumed that the power line conductor could be considered a straight line in the vicinity of the robot. However, it was later found that the inherent change of slope due to robot's weight could not be ignored, i.e., $\alpha \neq 0$ in Figure 14. Actual values are typically a few degrees but depend on local tension of the line and on the robot's location on the span. Based on Figure 14, the distance at which the LIDAR plan crosses the conductor (P_C) can be expressed as follows:

$$D_C = \frac{(P_{1X} - P_{0X})\tan\alpha - (P_{1Z} - P_{0Z})}{\sin\theta - \cos\theta\tan\alpha} \quad (2)$$

$$S_C = \frac{(P_{1X} - P_{0X}) + D_C\cos\theta}{\cos\alpha} \quad (3)$$

As seen in Figure 15, the Hokuyo UTM-30LX is mounted far below the conductor on a dedicated bracket with an adjustable angle. In this case, ($P_{1X} - P_{0X}$) = 0.39 m, and P_{1Z} = -0.61 m. This position does not interfere with the LineScout obstacle-crossing sequence and allows angle θ to be set between 25º and 50º, keeping S_C > 0.9 m.

Once the LIDAR starts collecting data, range filtering is applied in the angular range (±12º), which typically leaves N measurements (N = 49). Conductor edges are then identified by finding maximum slopes among the N points, i.e., the index for which the maximum (a) and minimum (b) variations of measurements occur. From that, the apparent conductor diameter D_0 is set to:

$$D_0 = D_m \cdot (b - a - 1) \cdot \delta \quad (4)$$

where D_m is the average distance returned by the LIDAR in the index range [*a, b*] and δ is the sensor's angular resolution (0.25º), expressed in radians. In this paper, the simplified algorithm proposed for obstacle detection is to constantly monitor results obtained with Eq. (4), to record and average those results for a few seconds on an obstacle-free section of the span, and then to detect any variation that exceeds the average by a certain threshold.

When encountering an obstacle, Eq. (3) is used to locate it relative to the center point of LineScout. For that purpose, an assumed constant value of α must be assessed upon stepping onto any new span, threw a calibration process that uses $D_C = D_m$ is used in Eq. (3) to calculate a value for α.:

$$\alpha = \tan^{-1}\left[\frac{D_m \sin\theta + (P_{1Z} - P_{0Z})}{D_m \cos\theta + (P_{1X} - P_{0X})}\right] \quad (5)$$

Figure 15. Mock-up for preliminary LIDAR validation testing

B. *Experimental Results*

The following sections present scans of three common obstacles encountered by LineScout on conductors. For each, detecting a variation in apparent diameter D_0 seems to be a viable approach. Furthermore, detecting a change in distance D_m could also be a powerful detection criterion.

1) *Vibration Damper Detection*

Vibration dampers (see Figure 3d) are installed near towers or at mid-span to damp wind-induced vibrations. Figure 16 shows that either criterion could be used to detect the obstacle since there is a clear variation on both graphs.

2) *Suspension Clamp Detection*

Suspension clamps support the conductor (Figure 3c). Their width varies from 75 to 220 mm and they are up to 2000 mm long. As with vibration dampers, either criterion is effective since the apparent diameter and distance both vary significantly (Figure 17).

3) *Conductor Splice Detection*

The last obstacle to be detected was a conductor splice (Figure 3f). Splices are about 1000 mm long, but only 5 to 8 mm larger in radius than the conductor, making them the most difficult obstacle to detect. Results presented in Figure 18 are very promising: the variation in apparent diameter is clear enough to permit detection. However, although changes also occur for D_m, the data collected is too noisy to use this criterion directly.

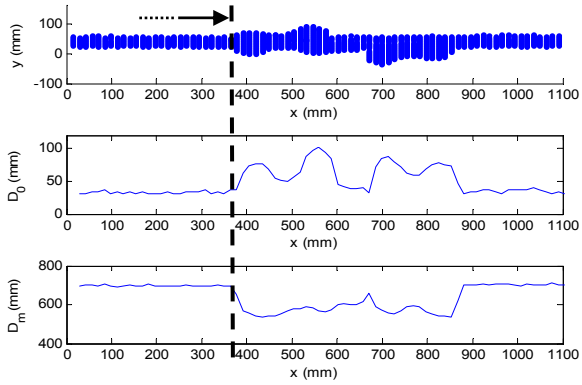

Figure 16. Vibration damper detection (scanning angle of 45˚)

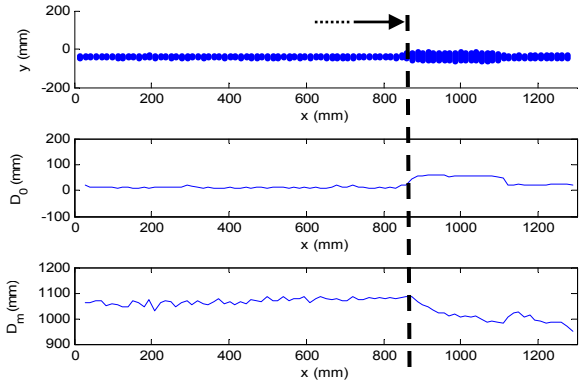

Figure 17. Clamp detection (scanning angle of 45˚)

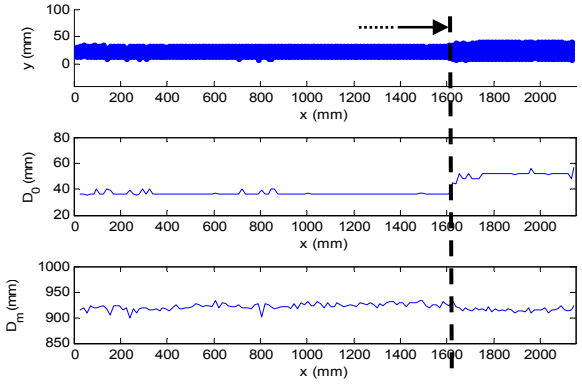

Figure 18. Splice detection (scanning angle of 45˚)

V. Conclusion & Future Work

We presented the initial phase of a multi-phase project to use LIDAR for the first time in the emerging field of power line robotic applications. One objective was to validate that the sensor chosen, the Hokuyo UTM-30LX, performed well enough to detect and localize common obstacles. To do so, we undertook its systematic characterization and focused on the novel application of conductor scanning. The following conclusions can be drawn:

- The UTM-30LX must be warmed up for 30 minutes for practical use.
- The effect of orientation on measurement error was $\leq 0.14\%$.
- The effect of vibrations on measurement error was $\leq 0.16\%$, for the amplitudes and frequencies studied.
- The distance evaluation error remains $< 1.2\%$ for cylindrical targets in the range of interest (500 to 1500 mm), with higher precision at 1000 and 1500 mm.
- Angular orientation of cylindrical targets influences the distance measurement but the distance evaluation error is $< 1\%$ for angles $\geq 40^{\circ}$ at distances of about 1000 mm.
- Obstacle localization algorithm has been developed.
- Various obstacles found on typical power lines can clearly be detected even the smallest one, a splice. Either the apparent diameter or distance can be used as a criterion, except for a splice where apparent diameter is preferable.

The next steps will involve outdoor testing to investigate the effect of varying light conditions (direct sunlight, shadows and shade) and more complex background (e.g., tower lattice structures). The effect of the strong electromagnetic field generated by high voltage and current on the line will also be assessed. Preliminary results for LIDAR signal intensity show that this parameter could further enhance the detection threshold or be used to evaluate the surface conditions of power line components.

ACKNOWLEDGMENTS

The authors would like to thank personally all development team members of the Institut de Recherche d'Hydro-Québec (IREQ). Thanks also to Hydro-Québec TransÉnergie personnel for their precious collaboration in this innovative and challenging project.

REFERENCES

[1] Toussaint, K., Pouliot, N. and S. Montambault, "Transmission Line Maintenance Robots Capable of Crossing Obstacles: State-of-the-Art Review and Challenges Ahead", Journal of Field Robotics, Wiley Ed., Vol. 26, No. 5, May 2009, pp. 477–499.

[2] S. Montambault and N. Pouliot, "LineScout Technology: Development of an Inspection Robot Capable of Clearing Obstacles While Operating on a Live Line", 11th Int. Conf. on Transmission and Distribution Construction, Operation and Live-Line Maintenance, ESMO 2006.

[3] N. Pouliot and S. Montambault, "Geometric Design of the LineScout, a Teleoperated Robot for Power Line Inspection and Maintenance", Proceedings of the IEEE Int. Conf. on Robotics and Automation, ICRA 2008, pp. 3970-3977.

[4] N. Pouliot and S. Montambault, "Field-oriented developments for LineScout Technology and its deployment on large water crossing transmission lines". Journal of Field Robotics, Wiley Ed., Vol. 29, No. 1, January 2012, pp. 25–46.

[5] N. Pouliot, P. Latulippe, S. Montambault, and S. Tremblay, "Reliable and Intuitive Teleoperation of LineScout: a Mobile Robot for Live Transmission Line Maintenance", Proceedings of the IEEE/RSJ Int. Conf. on Intelligent Robots and Systems IROS 2009, pp. 1703-1710.

[6] J. F. Peters, T. C. Ahn, and M. Borkowski, "Obstacle classification by a line-crawling robot: a rough neurocomputing approach", Rough Sets and Current Trends in Computing, Proceedings of the 3rd Int. Conf. (RSCTC 2002), Vol. 2475, pp. 594–601, 2002.

[7] J. F. Peters, S. Ramanna, and M. S. Szczuka, 2003, "Towards a Line-Crawling Robot Obstacle Classification System: A Rough Set Approach", RSFDGrC 2003, LNAI 2639, pp. 303–307.

[8] S. Fu, W. Li, Y. Zhang, Z. Linag, Z. Hou, M. Tan, W. Ye, B. Lian, and Zuo, "Structure-Constrained Obstacles Recognition for Power Transmission Line Inspection Robot", Proceedings of the 2006 IEEE/RSJ Int. Conference on Intelligent Robots and Systems, pp. 3363-3368.

[9] Z. Qi, X. Zhi, G. Zijian, and S. Dehui, "The obstacle recognition approach for a power line inspection robot", Int. Conf. on Mechatronics and Automation ICMA 2009, Aug. 9-12, 2009, pp. 1757-1761.

[10] S. Han and J. Lee, "Path-Selection Control of a Power Line Inspection Robot Using Sensor Fusion", IEEE Int. Conf. on Multisensor Fusion and Integration for Intelligent Systems, Aug. 20-22, 2008, pp. 8-13.

[11] G. Wu, T. Zheng, Z. Huang, H. Liu, and C. Li, "Navigation strategy for local autonomous obstacles-overcoming based on magnetic density detection for inspection robot of single split high voltage transmission line", 8th World Congress on Intelligent Control and Automation (WCICA), July 7-9, 2010, pp. 6555-6561.

[12] G. Wu, X. Xu, H. Xiao, J. Dai, X. Xiao, Z. Huang, L. Ruan, C. Xiong, and H. Liu, "A Novel Self-navigated Inspection Robot along High-Voltage Power Transmission Line and Its Application", ICIRA 2008, Springer Berlin / Heidelberg, pp. 1145-1154

[13] M. Frank, P. Zhihong, B. Raber, and C. Lenart, "Vegetation management of utility corridors using high-resolution hyperspectral imaging and LiDAR", 2nd Workshop on Hyperspectral Image and Signal Processing: Evolution in Remote Sensing (WHISPERS) 2010, pp. 1-4.

[14] R.V. Ussyshkin, L. Theriault, M. Sitar, and T. Kou, "Advantages of Airborne Lidar Technology in Power Line Asset Management", International Workshop on Multi-Platform/Multi-Sensor Remote Sensing and Mapping (M2RSM) 2011, pp. 1-5.

[15] M. Alwan, M. B. Wagner, G. Wasson, and P. Sheth, "Characterization of Infrared Range-Finder PBS-03JN for 2-D Mapping," Proceedings of the 2005 IEEE Int. Conf. on Robotics and Automation, 2005. ICRA 2005. , pp. 3936- 3941, 18-22 April 2005

[16] L. Kneip, F. Tache, G. Caprari, and R. Siegwart, "Characterization of the compact Hokuyo URG-04LX 2D laser range scanner", . IEEE Int. Conf. on Robotics and Automation ICRA 2009, pp.1447-1454, 12-17 May 2009

[17] C. Park, D. Kim, B.-J. You, and S.-R. Oh, "Characterization of the Hokuyo UBG-04LX-F01 2D laser rangefinder", RO-MAN, 2010 IEEE , Sept. 13-15, 2010, pp.385-390.

[18] J. Pascoal, L. Marques, and A. T. de Almeida, "Assessment of Laser Range Finders in Risky Environments", IEEE/RSJ Int. Conf. on Intelligent Robots and Systems, IROS 2008, Sept. 22-26, 2008, pp.3533-3538.

[19] K.-H. Lee and R. Ehsani, "Comparison of two 2D laser scanners for sensing object distances, shapes, and surface patterns", Computers and Electronics in Agriculture, Vol. 60, No. 2, March 2008, pp. 250-262.

[20] H. Tamura, T. Sasaki, H. Hashimoto, and F. Inoue, "Circle fitting based position measurement system using laser range finder in construction fields", IEEE/RSJ Int. Conf. on Intelligent Robots and Systems, IROS 2010, Oct. 18-22, 2010, pp. 209-214.

[21] M. W. McDaniel, T. Nishihata, C. A. Brooks, and K. Iagnemma, "Ground plane identification using LIDAR in forested environments", Proceedings of the IEEE Int. Conf. on Robotics and Automation ICRA 2010, May 3-7, 2010, pp. 3831-3836.